

Single hot thermocouple technique for the characterization of the crystallization behavior of transparent or translucent liquids

N. Kölbl · I. Marschall · H. Harmuth

Received: 24 June 2010/Accepted: 8 April 2011/Published online: 21 April 2011
© Springer Science+Business Media, LLC 2011

Abstract Both time–temperature-transformation (TTT) and continuous-cooling-transformation (CCT) diagrams have been established to characterize the crystallization behavior of slags in a selected temperature range. Therefore, the single hot thermocouple technique based on already existing equipment was constructed showing also some different approaches. Furthermore, the procedure was enhanced using a stretching device enabling the formation of very thin slag layers. This device permits the investigation of not only transparent but also translucent liquids with low amounts of coloring oxides, e.g. Fe₂O₃. For the initiation of this method, a transparent synthetic NCAS-slag showing a high crystallization tendency was used to proper adjust the control parameters. Afterward, two industrial mould slags for the continuous casting of steel were investigated and TTT- as well as CCT-diagrams created. The TTT-diagrams for both mould slags show only one nose but the shapes of crystals formed differ dependent on temperature. This is contributed to the ratio of the growth to nucleation rate which is raised at higher temperatures where dendritic crystals are formed. For the case of continuous-cooling experiments observing only the formation of dendritic crystals precipitating at temperatures close to the liquidus temperatures the same explanation is assumed. Contrary, this ratio is decreased for rather low temperatures where only fine separate crystals precipitate.

Introduction

In the continuous casting process, mould powders are added to the top of the liquid steel in the mould. In contact with the steel, a liquid slag is formed which is entrapped into the gap between the mould and the solidifying strand where three different layers are formed: a glassy one in contact with the mould, a crystalline layer in the middle and a liquid layer on the strand side. To describe the processes taking place in the mould, a lot of different investigation methods have already been implemented [1–7]. One of them is the Confocal Scanning Laser Microscope with a high temperature heating system. The He–Ne-laser of this microscope provides a sufficient contrast in spite of the thermal radiation of the specimen and enables a higher resolution at elevated temperatures. This equipment is mainly used for *in situ* observations of the crystallization behavior of slags or dissolution processes of different particles added to the slag [3]. Using the high temperature viscometer, it is possible to determine the Break Temperature often related with the crystallization of a liquid. This temperature is characterized by a sudden increase of the viscosity [4]. Furthermore, the simultaneous thermal analysis (STA) is used to detect crystallization during cooling by the associated exothermal peak [5]. To identify the phases formed during cooling, X-ray diffraction (XRD) was implemented. This may be performed either *in situ* with the help of a special heating unit or after quenching the specimens to room temperature [6, 7]. For the latter also microscopical investigations are applied. To enable visual *in situ* observation of the crystallization the hot thermocouple technique has been implemented [8]. Using this method, it is possible to obtain time–temperature-transformation (TTT) and continuous-cooling-transformation (CCT) diagrams to characterize the crystallization

N. Kölbl (✉) · I. Marschall · H. Harmuth
University of Leoben, Peter-Tunner-Straße 5,
8700 Leoben, Austria
e-mail: nathalie.koelbl@unileoben.ac.at

behavior of transparent slags. For these purposes, in most cases the single hot thermocouple technique where the slag is stretched within the loop of one thermocouple is used [9–12]. In order to observe the behavior of the slag under service conditions, the double hot thermocouple technique is applied. Due to the fact that the sample is stretched between two thermocouples being controlled independently from each other a temperature gradient can be applied [13, 14].

The hot thermocouple technique

Construction of the investigation device

The experimental setup was designed and constructed according to Cramb [8] with only minor modifications. The hot thermocouple technique consists of a furnace chamber including a heating unit, a stand with camera and objective, a controller and an image recording. The set up is shown in Fig. 1.

The furnace is made from a stainless steel block with an edge length of 70 mm and a height of 50 mm. Into the cylindrical furnace chamber situated in the centre of this steel block heating units are inserted through two horizontal bore holes. Further bore holes one on each of the other lateral faces allow gas purging during experimental procedure. The top of the chamber can be closed by a quartz window preventing the objective from precipitation of evaporating components. To proper adjust the heating units in the furnace under the objective, a manual x/y-table is used.

The heating unit for the single hot thermocouple technique inserted laterally into the heating chamber is



Fig. 1 Set up of the Hot Thermocouple Technique: 1 furnace chamber including heating units, 2 stand with camera and objective, 3 control PC, 4 control unit, and 5 PC for image recording

illustrated in Fig. 2. Into the insulating bar, copper tubes are inserted sticking out on both sides. On one end a platinum rhodium wire (Pt/Rh 70/30) bent into loop shape is mounted using spring clips, on the other side banana plugs are fixed to connect it to the power supply. Contrary to the equipment of Cramb [8], the platinum wire and the thermocouple have been separated; thus the thermocouple is not applied for heating the specimen. According to Fig. 2a close to the head of the platinum rhodium loop a type S thermocouple is situated which is in direct contact with the sample. The ends of the thermocouple wires are connected to the associated interface. In order to obtain an unimpaired view of the sample during experimental procedure, the wires of the thermocouple are directed out of the chamber via another insulating bar arranged oppositely.

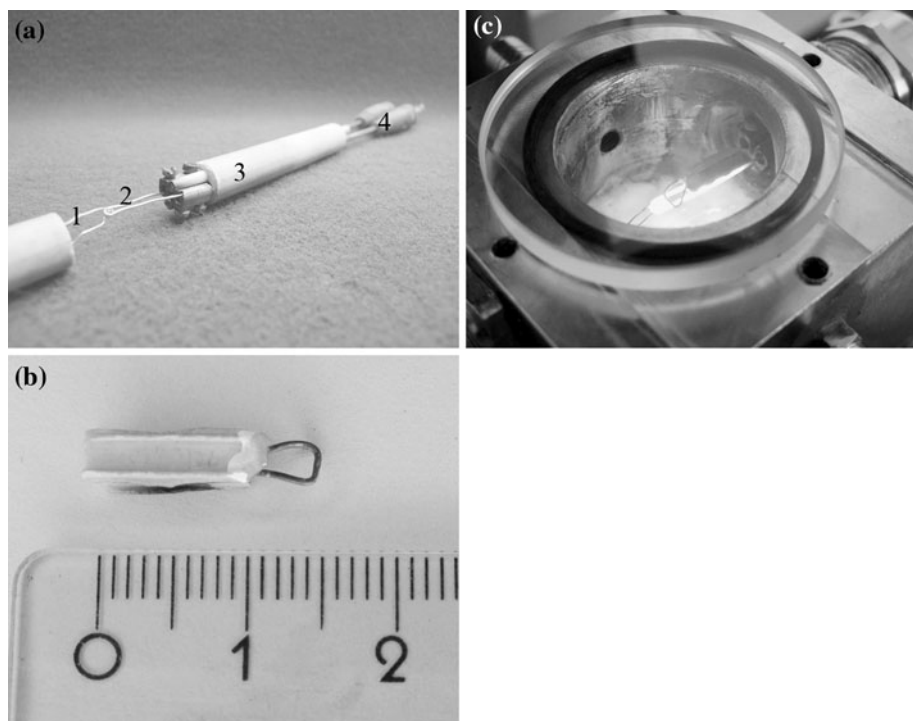
The image acquisition of the sample during the whole experimental procedure is carried out by a FireWire color camera; a telecentric objective with an adjustable aperture is mounted. Both camera and objective are fixed to the stand using a special mounting support. A spindle drive with shaft joint enables the focusing of the sample. Additionally, band-elimination filters and neutral gray filters are available which especially at high temperatures prevent from capturing overexposed pictures.

Temperature control and data recording

The temperature control is carried out by PID controllers, but also manual control is possible. In both cases, the triggering of the heating is carried out using pulse width modulation. For each heating unit, a 12VDC/300 W mains adapter is used as a voltage source. The series resistor upstream of the heating wire has a value of $4.7\ \Omega$. A Power MOSFET IRL 2505 is the actuating element which gets the information concerning the ratio of heating and idle period from the controlling PC via interface. This ratio called duty cycle rises with increasing power requirement.

The temperature of the sample taken from the loop head of the platinum rhodium wire using a type S thermocouple is the input parameter of the controlling PC. A special interface for importing temperature data transfers them to the PC. There, the actual control takes place using a program on the basis of the programming environment of “National Instruments” which was specially developed for this purpose. The user interface enables an immediate operation of the controlling parameters, for e.g. PID parameters. The input of the temperature profile is given by the heating rate in $^{\circ}\text{C}/\text{min}$ and the maximum temperature in the intended input fields. Based on these values, the temperature is adjusted via PID control. The setpoint already entered can be modified during the experimental procedure according to the requirements. Another option to set the temperature is the manual temperature control. In this case,

Fig. 2 Details of the experimental design: **a** heating unit, **b** heating device before, and **c** during operation



the value for the duty cycle is chosen by scrolling the slider to the desired value.

To prevent the heating wire from fusion due to a too high current flow in the case of using PID control, the maximum allowable duty cycle can be limited. This limit may be changed during operation in case the setpoint cannot be attained with the maximum power available.

Via network, the controlling PC is connected to another one being responsible for the image recording. For this purpose also, a program has been developed using LabVIEW® merging the image data from the camera and the temperature information of the controlling PC and saving a video afterward. The user interface enables the camera control concerning color balance, contrast and brightness, and the positioning of the temperature values within the graphical representation. The data exchange is carried out using DataSocket® which is an integrated interface in LabVIEW® for application programs. To display both the visual and the temperature information, another LabVIEW® program (AVI-Reader) has been applied.

Initial operation

Due to the fact that the design of the software enables the individual adaption of most parameters (PID parameter and software based parameters), this values have to be evaluated before the hot thermocouple technique can be used for investigations. If this is not the case, the function as well as the stability of the control is not provided. The controller optimization was carried out according to Ziegler–Nichols

[15]. For this procedure, the control circuit is closed using only the proportional controller. Afterward, the current is increased until the output of the controlling circuit shows a continuous oscillation with a period of T_{crit} and a controller gain $K_{p, \text{crit}}$. Based on these values, the PID parameters can be estimated.

The first tests were carried out using a synthetic NCAS-slag (see Table 1). This slag was chosen because of its very transparent melt which may be easily distinguished from the crystals precipitated. After preparation as described below, the sample is heated until a homogeneous liquid is formed. Due to the fact that the platinum rhodium wire is wetted by the slag, a droplet with a diameter of 2–3 mm is formed at the end of the loop. However, because of the high transparency the crystallization can be observed, but an analysis regarding the crystalline fraction is not possible. Therefore, a special device (Fig. 2) was implemented to stretch the slag over a larger area. A piece of a platinum wire was bent to a small loop and fixed in a ceramic tube with square section for galvanic separation. This device is positioned on the platinum rhodium wire. After liquefaction the slag is contacted with the platinum wire of the stretching device which is then moved in radial direction to the furnace wall. Thus, a thin slag film is formed.

While the presetting of a constant cooling rate for the creation of continuous-cooling transformation (CCT) diagrams does not pose a problem, the quenching to defined temperatures is more difficult. It is not possible to quench the sample to the desired temperature automatically because the control algorithm is not suitable for such high cooling rates. Therefore, this has to be done manually. If

Table 1 Chemical composition of the investigated synthetic slag NCAS and of two mould powders MP 1 and MP 2 (in wt%)

| | NCAS | MP 1 | MP 2 |
|--------------------------------|------|-------|-------|
| F | | 5.42 | 8.01 |
| Na ₂ O | 6 | 8.4 | 7.67 |
| MgO | | 3.09 | 1.37 |
| Al ₂ O ₃ | 4 | 5.19 | 3.00 |
| SiO ₂ | 45 | 38.19 | 31.17 |
| P ₂ O ₅ | | 0.08 | 0.93 |
| SO ₃ | | 0.27 | 0.45 |
| K ₂ O | | 0.52 | 0.14 |
| CaO | 45 | 31.39 | 41.91 |
| TiO ₂ | | 0.11 | 0.03 |
| Cr ₂ O ₃ | | 0.03 | |
| MnO | | 0.04 | 0.06 |
| Fe ₂ O ₃ | | 1.71 | 0.41 |
| ZrO ₂ | | | 0.11 |
| BaO | | 0.09 | 0.03 |
| B ₂ O ₃ | | 0.12 | |
| C | | 5.34 | 4.71 |
| C/S | 1 | 0.82 | 1.34 |

only the energy supply is reduced a sufficiently rapid cooling cannot be achieved. Thus, an additional device is necessary to cool the whole furnace chamber. A suction bulb is connected to the bore for the gas inlet to realize a higher cooling rate. Via air blasts the slag is quenched to the desired temperature. Trials to use the automatical control in combination with the suction bulb failed due to the fact that an air blast causes a major change of the input parameter resulting in an oscillation of the control. Another option to switch to PID control after the desired temperature has been achieved was tested too. But this operation always yields to a spontaneous increase of temperature. Therefore, the target temperature is also kept constant via manual control. Based on this procedure, cooling rates of about 100 °C/s can easily be achieved.

Experimental procedure

Sample characterization

Chemical compositions of slags investigated are given in Table 1.

Sample preparation

Several preparation techniques have been experienced. At the beginning of the implementation of the hot thermocouple technique the mould powder was mixed with

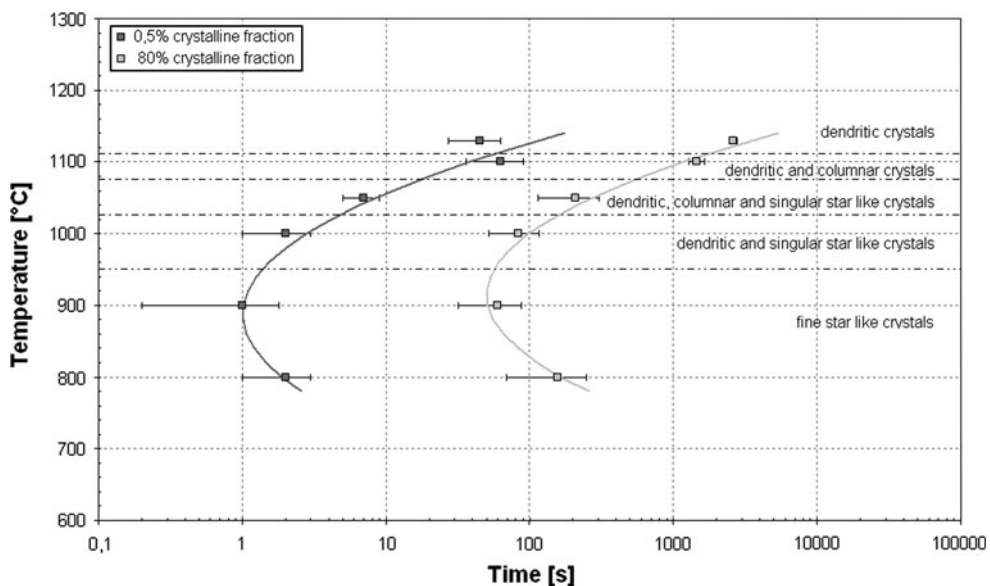
alcohol in a laboratory vessel in such a ratio that a papescent mass was gained. A small amount of this mass was applied to the platinum rhodium wire and heated to the formation temperature of a homogeneous melt. Due to the fact that already during heating up alkalis evaporate the sample preparation was modified. The papescent mass was applied to the wire after the maximum temperature was reached. Since the alcohol evaporated spontaneously when the mass was inserted into the preheated chamber, the sample could not be placed on the wire. Then, the mould powder was pressed to pills 2 mm in height without using any kind of a binder. From these pills, samples were cut which were afterward applied to the preheated wire.

Isothermal and continuous-cooling experiments

For both types of measurements, the pressed original mould powder is applied to the heating wire after reaching the maximum temperature. There it is melted and afterward stretched using the special device quoted above. Then, the furnace chamber is closed by a quartz window and the objective is adjusted. In the case of the isothermal experiments, the sample is quenched to the desired temperature immediately using the manual control to decrease the electrical power and the suction ball to cool the chamber with air blasts. After achieving the desired temperature it is held constant. The temperature range for the investigation of the crystallization behavior of a mould slag is on the one hand limited by the melting temperature and on the other hand by the transparency of the sample. The more transparent a slag film the easier crystals can be distinguished from the residual melt and crystalline fraction can be determined. In case of slags with poor transparency, observation of first crystal formation at rather high or rather low temperatures is hindered by too intensive or insufficient radiation. The temperature range investigated is 800–1,100 °C for the slag of MP 1 and 800–1,120 °C in the case of MP 2. Contrary to this for the continuous-cooling experiment, the slag is cooled with a constant cooling rate using the automatical control. The cooling rates used are 5, 10, 20, and 50 °C/min.

In the case of mould powders, care must be taken to ensure that the chemical composition of the slag is not changed during the experiment due to the evaporation of alkalis and fluorine. Otherwise, a slag differing from the original one would be investigated. One can counteract this by reducing the maximum temperature to a value where a homogeneous liquid is barely formed and by a certain skill during stretching the sample which leads to a lower dwell time at the maximum temperature. But this procedure is only useful if the sample is cooled with higher cooling rates afterward. If this is not the case volatile contents will vaporize until a certain temperature is reached. Therefore, CCT experiments should not be performed with too low cooling rates.

Fig. 3 TTT-diagram of the mould slag of MP 1



Data evaluation

For data evaluation the videos of the experimental procedures are used applying the AVI-Reader. This software enables the selection of single pictures which may then be processed by an image editor. Since crystals cannot automatically be distinguished from the residual liquid a manual coloring of the picture is necessary. The edited picture can then be analyzed using a program which enables the calculation of the crystalline fraction based on the determination of the number of pixels of each color. The crystalline fraction determined by this procedure has to be considered to be a nominal quantity as the crystalline fraction of the crystallized area itself is usually below 100%. This is caused by liquid phase present, for e.g., between the branches of dendrites. To evaluate the crystalline percentage of the crystallized area, a polished sample of its cross section has to be investigated using reflected light and scanning electron microscopy.

In literature, the start of the crystallization is characterized by 0.5% crystallinity and the end by 95% [10]. But the mould slags investigated in this paper do not show 95% crystallinity for all temperatures after a significant dwell time. For this reason, the TTT-curves are given for 0.5 and 80% crystalline fraction.

Results and discussion

TTT-diagrams

Crystallization of the synthetic NCAS-slag occurs so rapidly that a TTT-curve for 0.5% crystalline fraction could not be determined. Only the curves of higher crystallinity

(>10% crystallinity) can be created. Over the whole temperature range between 1,000 and 1,220 °C the formation of dendritic crystals is observed. These solidify not only in contact with the loop but also in contact with the stretching device. Both crystalline fronts move toward each other rapidly during dwell time. Within a few seconds the whole stretched area is crystallized. Also, the results of the mould powders show that the first crystals are formed rapidly after the desired temperature is reached. At temperatures close to the nose temperature, the crystallization takes place in such a short time that the application of the suction bulb enhancing the cooling rate is necessary.

In the case of mould slags depending on the desired temperature different crystal shapes are formed. This enables the partition of the TTT-diagram of MP 1 into five zones (Fig. 3). At temperatures above 1,100 °C, the crystallization of dendrites is observed. In the temperature range between 1,070 and 1,110 °C, not only dendritic but also columnar crystals are formed. While between 950 and 1,020 °C, dendritic and separate faceted crystals solidify, below 950 °C only very fine single crystals showing a dendritic growth with increasing dwell time separate from the liquid. A comparison of the different crystal shapes at 850 and 1,100 °C is given in Fig. 4.

The investigation of the second mould powder MP 2 results in TTT-curves showing also one nose. But in this case only a division into three sections according to the three morphologies observed is possible: at temperatures above 970 °C, the crystallization of dendritic crystals and below 870 °C of very fine separated crystals takes place. In-between single faceted crystals solidify. The reason for the lack of columnar crystals could not be identified.

This classification of the TTT-diagram into different areas has also been reported by Orrling et al. [11, 12]. It

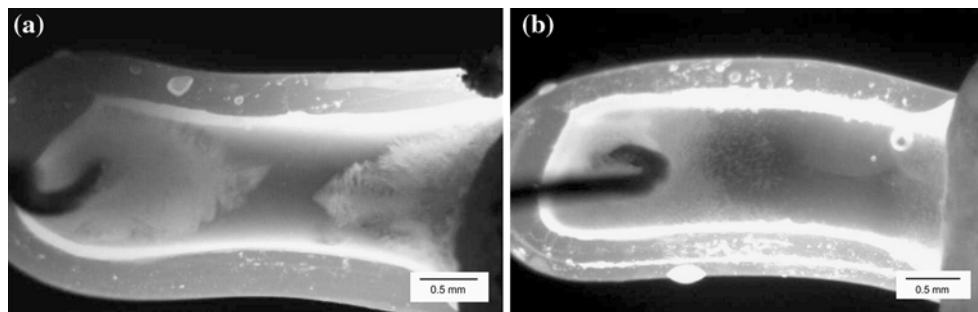


Fig. 4 Illustration of the crystallization behavior of the mould slag of MP 1 after quenching to **a** 1,100 °C and **b** 850 °C

can be assumed that the different morphologies depend on the ratio of the growth to nucleation rate: in the case of dendritic crystals formed via interface nucleation in contact with the platinum wire this ratio tends to be high. Otherwise, for the crystallization of single-faceted crystals the ratio is reduced and bulk nucleation takes place. Similar morphologies have been detected in samples taken from service. In the slag films at the mould side where the slag is assumed to be quenched to lower temperatures single crystals are formed, whereas in the direction to the strand their morphologies change to dendritic.

Crystals precipitating via volume nucleation show a high specific crystal/slag interface surface area compared to dendritic ones. In case of the same crystalline volume fraction, it is supposed that this fact leads to an increase of the scatter of infrared radiation reducing the infrared transparency in turn. Some valuable results follow from an investigation of Hayashi et al. [16]. These authors observed especially a smaller heat flux in case of higher width of dendrites. This finding was explained by the Mie effect. Scattering of radiation by these dendrites was considered to be the main impact on heat flux. Further considering the friction increase it is supposed that single faceted crystals tend to result in lower friction compared to dendritic ones.

In the case of isothermal experiments for temperatures not close to the nose temperature of the TTT-diagram a 95% crystalline area could not be achieved for acceptable test duration. Therefore, it is not possible to establish a TTT-curve for 95% crystallinity for the total investigated temperature range. Instead the curve for 80% crystalline area observed for all steps is selected. Furthermore, considering the crystallized area it is most likely that its crystalline fraction is lower than 100%. Therefore, the TTT-diagrams given in this paper represent a nominal crystalline fraction. To estimate the crystallinity within this area further investigations have to be carried out.

CCT-diagrams

If the slag is cooled constantly using defined cooling rates a CCT-diagram according to Fig. 5 can be obtained. Here,

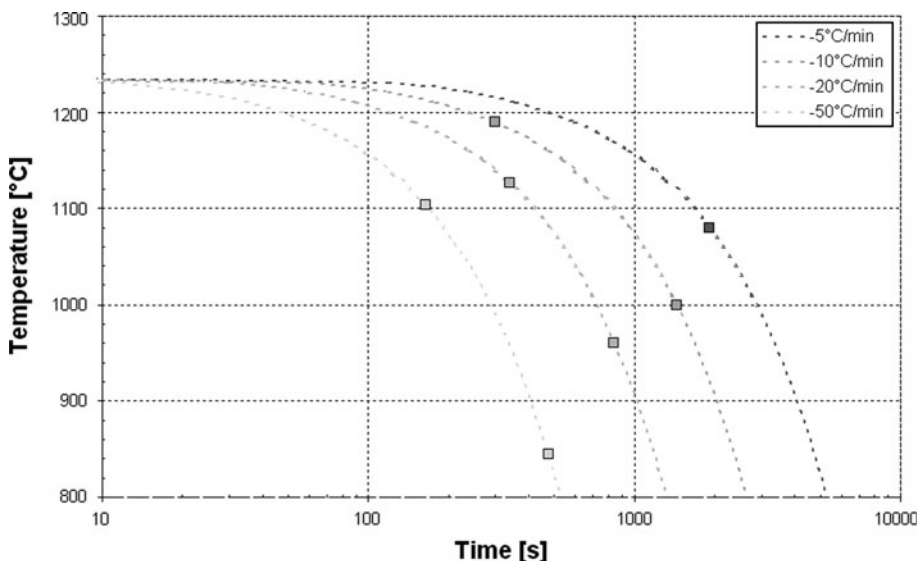
the onset and the end of crystallization can be seen. Independent of the cooling rate, dendritic crystals are formed for each of both mould slags in contact with the loop as well as in contact with the stretching device. Yet, using lower cooling rates the formation of considerable finer dendrites can be observed. It could be noticed that the formation of the first crystals was more difficult to detect for lower cooling rates. In the case of MP 1, it was even impossible to determine the start of crystallization for the cooling rate of 5 °C/min. Probably this is due to the formation of very fine dendrites which could not be detected with the magnification available.

The method

The results of these investigations demonstrate that the Single hot thermocouple technique is a powerful method to describe the crystallization behavior of transparent or translucent slags by calculating TTT- and CCT-diagrams. In the case of slags with poor transparency, it was necessary to provide a special device additional to that of Cramb et al. [8] for stretching the specimen. This tool enables the formation of a very thin slag film instead of a slag droplet not allowing the observation of the crystallization behavior within the slag. Mold slags may contain iron and manganese oxide which largely reduce transparency and impede observability of crystallization. This may be overcome by purging the specimen chamber with a reducing gas mixture, e.g. argon/hydrogen. Then, these oxides can be reduced to the metallic state. This is in accordance with service conditions, where these oxides are reduced due to the low prevailing oxygen partial pressure.

Comparing the TTT- and CCT-diagrams of one and the same slag, it is obvious that for the latter always a higher crystallinity is observed. This can be explained by the fact that for continuous-cooling experiments at least for not too high cooling rates crystallization takes place at rather high temperatures mainly in the vicinity of the growth rate maximum after nucleation at the interface. Therefore, conditions for total crystallization are rather favorable.

Fig. 5 CCT-diagram of the mould slag of MP 1



Conclusions

Based on the results and the equipment of Cramb et al. [8], the hot thermocouple technique was constructed and implemented for the characterization of the crystallization behavior of mould slags. During parameter evaluation and initial operations using a synthetic NCAS-slag with high transparency, the procedure of the experiments was enhanced also enabling the investigation of translucent slags. Based on this improvement for two mould slags, isothermal and continuous-cooling experiments were carried out to create TTT-diagrams for 0.5 and 80% crystalline fraction being the highest crystallinity achieved in a suitable time for temperatures above and below the nose temperature. Both TTT-diagrams are C-shaped and can be divided into different sections depending on the crystal shapes formed at certain temperatures. For one mould slag the division into three, for the other one into five sections is possible. Furthermore, the onset and the temperature of the end of crystallization have been depicted in CCT-diagrams. During all continuous-cooling experiments of both samples, only the crystallization of dendrites which were finer in the case of lower cooling rates could be observed. An explanation for the different morphologies of the crystals precipitating is based on the ratio of the growth to nucleation rate which tends to increase with rising temperatures.

Acknowledgements The research program of the competence center “Advanced Metallurgical and Environmental Process Development” (K1-MET) is supported within the Austrian program for competence centers COMET (Competence Center for Excellent Technologies) with funds of the Federal Ministry for Transport, Innovation and Technology, the Federal Ministry of Economy, the Province of Upper Austria and Styria, the Styrian Business Promotion Agency, of the Tyrol and the Tyrolian Future Foundation. We

gratefully acknowledge this support. Further, we thank A. W. Cramb for generously providing his know-how regarding the experimental setup.

References

- Watanabe K, Murakami K, Kondo H, Miyamoto A, Shiomi T (1997) NKK Tech Rev 77:20
- Singh D, Bhardwaj P, Yang YD, McLean A, Hasegawa M, Iwase M (2009) In: Proceedings of the VIII international conference on molten slags, fluxes and salts, p 1073
- Valdez M, Prapakorn K, Cramb AW, Sridhar S (2001) Steel Res 72:291
- Sridhar S, Mills KC, Afrange ODC, Lörz HP, Carli R (2000) Ironmak Steelmak 27:238
- Gronebaum RH, Pischke J (2007) Stahl Eisen 127:51
- Kromhout JA, Liebske C, Melzer S, Kamperman AA, Boom R (2008) In: Proceedings of the 6th European conference on continuous casting
- Kromhout JA, van der Plas DW (2002) Ironmak Steelmak 29:303
- Kashiwaya Y, Cicutti CE, Cramb AW, Ishii I (1998) ISIJ Int 38:348
- Kashiwaya Y, Cicutti CE, Cramb AW (1998) In: 81st Steelmaking conference proceedings, p 185
- Orrling C, Tilliander A, Kashiwaya Y, Cramb AW (1999) In: 82nd Steelmaking conference proceedings, p 417
- Orrling C, Cramb AW, Tilliander A, Kashiwaya Y (2000) Ironmak Steelmak 27:53
- Cramb AW (2010) Quantifying the thermal behaviour of slags. <http://www.osti.gov/bridge/purl.cover.jsp;jsessionid=3D07E0497A02C0F760333369CAF701F4?purl=/840954-t2Utds/native/>. (status: May 2010)
- Kashiwaya Y, Nakauchi T, Pham KS, Akiyama S, Ishii K (2007) ISIJ Int 47:44
- Lachmann S, Scheller P (2008) In: Proceedings of the 6th European conference on continuous casting
- Ziegler JG, Nichols NB (1942) Trans ASME 64:759
- Hayashi M, Matsuo K, Nagata K, Nakda H (2009) In: VIII International conference on molten slags, fluxes and salts, p 1091